

“Ordering in Bio-inorganic Hybrid Nanomaterials Probed by In Situ Scanning Transmission X-ray Microscopy”

Supporting Information

Jonathan R. I. Lee, Michael Bagge-Hansen, Ramya Tunuguntla, Kyunghoon Kim, Mangesh Bangar, Trevor M. Willey, Ich C. Tran, David A. Kilcoyne, Aleksandr Noy, and Tony van Buuren.*

Supporting Materials and Methods

Modeling Details

The expected relative intensities from the C=C π^* for horizontal and vertical wire orientations along and orthogonal to the electric field of the incident radiation, respectively, were modeled using a brute-force building-block-style approach. A series of n vectors representing C=C bonds were placed radially around the circumference of a nanowire at angles β . Each of the n vectors were considered at different polar, θ angles (defined by the index, q) and different azimuthal, φ angles (defined by the index, f). This 3-dimensional matrix, for a wire along the x-axis, is given by:

$$B_{n,q,f} = R_x(\beta_n) \cdot R_x(-90^\circ) \cdot \begin{pmatrix} \sin(\theta_q) \cdot \cos(\varphi_f) \\ \sin(\theta_q) \cdot \sin(\varphi_f) \\ \cos(\theta_q) \end{pmatrix}$$

Where B is the axis of the C=C bond and R_x is the rotation matrix about the x-axis:

$$R_x(\theta) = \begin{pmatrix} 1 & 0 & 0 \\ 0 & \cos(\theta) & -\sin(\theta) \\ 0 & \sin(\theta) & \cos(\theta) \end{pmatrix}$$

The transition dipole moments for the C=C π^* were modeled by finding three vectors in a plane perpendicular to the bond axis, each separated by 120° .

The measured reduction in transmission for many wires at the diameter was about 5/6, leading to transmission estimation by the Beer-Lambert Law at any given n^{th} molecule around the circumference of the wire to be:

$$T_n = e^{-\ln(6/5) \cdot |\sin(\beta_n)|}$$

Where T_n is the transmitted intensity for the n^{th} molecule.

Incorporating this transmission, the total intensity of the C=C π^* intensity, I , of an ensemble of bonds around a wire that adopt a particular θ_q and φ_f orientation, is:

$$I_{q,f} = \sum_n |E \cdot M_{n,q,f}| \cdot T_n$$

where $M_{n,q,f}$ represents the TDMVs that are in the plane orthogonal to the C=C bond axes at a given θ and φ on the surface of the wire, and we have summed over the molecules/bonds around the circumference of the wire. For horizontal wires, the electric field and wire are both left along the x-axis. For vertical wires, $\underline{\mathbf{E}}$ is now orthogonal to the wire, and this can be computed (equivalently) by either changing the $\underline{\mathbf{E}}$, or rotating the wire. As this result is only proportional to the intensity, the ratios of the intensities of horizontal to vertical wires are presented in the plots.

Beam Damage

Before analysis of the C=C bond orientation, it was necessary to account for the possibility that changes in the C=C π^* resonance arise from beam damage. The absorption of soft x-rays and interaction with low energy electrons emitted following photoabsorption by the sample substrate are well-known sources of beam damage in organic molecules, typically via bond-breaking and the associated double bond formation and/or cross-linking with neighboring molecules^[1, 2]. Spectroscopically, the beam damage manifests as an increase in the intensity of the C=C π^* resonance. While beam damage inevitably occurs during the STXM measurements of the DOPC-coated Si NWs, this beam damage is categorically not responsible for the observed differences in C=C π^* resonance intensity for the following reason: only data collected under identical experimental conditions (specifically the same sample, under equivalent exposure times - ≤ 10 ms per pixel - and, preferably, within the same field of view) were compared. Therefore, the beam damage should be identical for each stack and cannot account for *differences* in the π^* intensity. In addition, we note that the intensity of the C=C π^* resonance at high α falls well below the intensity reported in the literature and for the DOPC standard measured in this study, which indicates that any beam damage is limited; in fact, comparison of XAS spectra derived

from consecutive stacks recorded on DOPC-coated Si NWs reveal an increase in the π^* resonance of intensity of $\sim 50\%$ over the course of an entire stack plot. Since the π^* resonance intensity is measured at $\sim 40\%$ into the stack, beam damage is unlikely to account for more than 20% of the total π^* signal in the first of the consecutive stacks, if one assumes that the damage follows first order kinetics and increases in a linear fashion with applied dose^[3].

STXM studies of polymers also illustrate that the intensity of the C=O π^* resonance provides an additional, high sensitivity, marker of beam damage^[2-4]. For films of polymers such as PMMA, which is reported to be more sensitive to beam damage than lipids^[5], the intensity of the C=O π^* resonance rapidly diminishes with irradiation. As the XAS data displayed in figure 5 of the main manuscript demonstrates, the C=O π^* resonance for the phospholipid layers on the Si NWs retains a high intensity (consistent with spectra reported in the literature for largely undamaged phospholipids). As a consequence, the exposure during a stack must fall well below the critical dose threshold for these materials (the dose require to reduce the resonance intensity to $1/e$)^[3, 4]

Method for calculating relative DOPC layer thicknesses

The relative thicknesses of the DOPC layers formed on distinct regions of the Si NWs (specifically the Si NWs versus nodes made by two wires touching) were calculated using a well-defined method, which is based upon comparison of the transmitted x-ray intensities from different regions of the experimental samples. The transmitted intensity will follow the Beer-Lambert law:

$$(1) \quad T = \frac{I}{I_0} = e^{-\mu t}$$

where T is the transmission, I_0 is the incident intensity, I is the measured signal, μ is the element-specific linear absorption coefficient, and t is the sample/material thickness. In our multi-component system, we define three distinct regions: (i) through solution only, (ii) through a single lipid-coated Si NW, suspended in solution, and (iii) nodes where two or more Si NWs intersect. The transmitted signal through the solution only, region (i), is used to approximate I_0 for regions (ii)-(iii). This is reasonable given that the solution is believed to be $\sim 1 \mu\text{m}$ thick, which is much greater than the diameter of the wires ($\sim 50\text{-}100 \text{ nm}$).

From a complete energy stack, we confine our analysis to energies well above and below the C K-edge at 280 and 300 eV, respectively. At 280 eV, Si dominates absorption of photons directed through the Si NW such that we make the approximation:

$$(2) \quad \mu \approx \mu_{Si}$$

$$(3) \quad T_{280,wire} = e^{-\mu_C t_C} \cdot e^{-\mu_{Si} t_{Si}} \approx e^{-\mu_{Si} t_{Si,w}}$$

$$(4) \quad T_{280,node} = e^{-\mu_C t_C} \cdot e^{-\mu_{Si} t_{Si}} \approx e^{-\mu_{Si} t_{Si,n}}$$

Where the subscripts C and Si denote the corresponding elements and the subscripts w and n correspond to the wire and node respectively. At 300 eV, (2) is no longer suitable. We can express the transmission for the wire and node as:

$$(5) \quad T_{300,wire} = e^{-\mu_C t_{C,w}} \cdot e^{-\mu_{Si} t_{Si,w}}$$

$$(6) \quad T_{300,node} = e^{-\mu_C t_{C,n}} \cdot e^{-\mu_{Si} t_{Si,n}}$$

If we further assume that $\mu_{Si,300} \approx \mu_{Si,280}$ we can combine (3)-(6) to solve for the ratio of carbon

thickness on the wire/node:

$$(7) \quad \frac{t_{c,w}}{t_{c,n}} \cong \frac{\ln[T_{280,wire}] - \ln[T_{300,wire}]}{\ln[T_{280,node}] - \ln[T_{300,node}]}$$

Relative Intensity Maps

Figure S1(a) displays a relative intensity map obtained for DOPC coated Si NWs at the Si *K*-edge by taking the natural logarithm of the intensity ratio for each individual pixel of aligned STXM images collected above and below the absorption onset, specifically at 1850 and 1830 eV respectively (i.e. the signal of each pixel in figure S1(a) is $-\ln(I_{h\nu=1850\text{eV}}/I_{h\nu=1830\text{eV}})$). The raw images used in deriving the map in figure S1(a) are displayed in figures 2(a) and (b) in the main manuscript. The rod-like features observed in figure 2(b) of the main manuscript are clearly evident as bright features in figure S1(a), thereby confirming that they are Si-based.

A comparable map obtained at the C *K*-edge for the images displayed in figures 3(a) and (b) of the main manuscript is displayed in figure S1(b). In this instance, the signal at each pixel corresponds to the natural logarithm of the pixel intensity at 280 and 300 eV (below and above the absorption edge respectively), i.e. $-\ln(I_{h\nu=300\text{eV}}/I_{h\nu=280\text{eV}})$. The structure of the bright features is consistent with (1) the presence of a carbonaceous layer on the surface of the Si NWs and (2) that this layer is significantly thicker at the points of contact (nodes) between these wires.

Figure S1(c) displays a relative intensity map obtained at the C *K*-edge for an uncoated Si NW using the same method described for figure S1(b). The raw images used in deriving the map in figure S1(c) are displayed in figures 3(c) and (d) of the main manuscript. It is evident that no features are resolved in figure S1(c), which supports the assignment that there is little or no carbonaceous coating on the surface of the NWs.

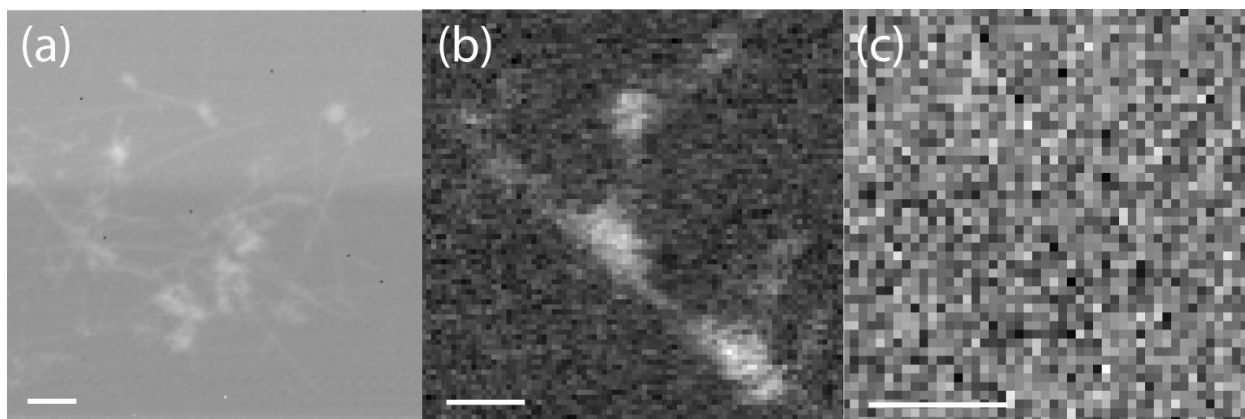


Figure S1. (a) Map of DOPC-coated Si NWs obtained via comparison of each pixel intensity from aligned STXM images (specifically those displayed in figure 2(a) and (b) of the main manuscript) obtained above ($h\nu = 1850$ eV) and below ($h\nu = 1830$ eV) the Si *K*-edge. The signal at each pixel corresponds to $-\ln(I_{h\nu=1850\text{eV}}/I_{h\nu=1830\text{eV}})$. Maps of (b) DOPC-coated Si NWs and (c) bare Si NWs obtained via comparison of each pixel intensity from aligned STXM images (specifically those displayed in figure 3(a) and (b) and figures 3(c) and (d) of the main manuscript) obtained above ($h\nu = 300$ eV) and below ($h\nu = 280$ eV) the C *K*-edge. The signal at each pixel corresponds to $-\ln(I_{h\nu=300\text{eV}}/I_{h\nu=280\text{eV}})$. The scale bars correspond to $1\mu\text{m}$ in (a) and 400 nm in (b) and (c). The intensity in each map is normalized to a linear grayscale in which the brightest pixel is assigned a signal of 100 (white) and the darkest in assigned a signal of 0 (black).

References

- [1] M. Zharnikov, W. Geyer, A. Golzhauser, S. Frey, M. Grunze, *Physical Chemistry Chemical Physics* 1999, 1, 3163; M. Zharnikov, M. Grunze, *Journal of Vacuum Science & Technology B* 2002, 20, 1793.
- [2] E. G. Rightor, A. P. Hitchcock, H. Ade, R. D. Leapman, S. G. Urquhart, A. P. Smith, G. Mitchell, D. Fischer, H. J. Shin, T. Warwick, *Journal of Physical Chemistry B* 1997, 101, 1950.
- [3] J. Wang, C. Morin, L. Li, A. P. Hitchcock, A. Scholl, A. Doran, *Journal of Electron Spectroscopy and Related Phenomena* 2009, 170, 25.
- [4] J. Wang, G. A. Button, M. M. West, A. P. Hitchcock, *Journal of Physical Chemistry B* 2009, 113, 1869.
- [5] B. O. Leung, A. P. Hitchcock, A. Won, A. Ianoul, A. Scholl, *European Biophysics Journal with Biophysics Letters* 2011, 40, 805.